HHS Public Access

Author manuscript

Neurobiol Aging. Author manuscript; available in PMC 2023 January 01.

Published in final edited form as:

Neurobiol Aging. 2022 January ; 109: 113–124. doi:10.1016/j.neurobiolaging.2021.09.012.

Age-related alterations to working memory and to pyramidal neurons in the prefrontal cortex of rhesus monkeys begin in early middle-age and are partially ameliorated by dietary curcumin

W. Chang[1], **C.M. Weaver**[2], **M. Medalla**[1], **T.L. Moore**[1], **J.I. Luebke**[1,*]

[1]Department of Anatomy & Neurobiology, Boston University School of Medicine 650 Albany St., Boston MA 02118 USA

[2]Department of Mathematics, Franklin and Marshall College, Lancaster PA 17604 USA

Abstract

Layer 3 (L3) pyramidal neurons in aged rhesus monkey lateral prefrontal cortex (LPFC) exhibit significantly elevated excitability *in vitro* and reduced spine density compared to neurons in young subjects. The time-course of these alterations, and whether they can be ameliorated in middle age by the powerful anti-oxidant curcumin is unknown. We compared the properties of L3 pyramidal neurons from the LPFC of behaviorally characterized rhesus monkeys over the adult lifespan using whole-cell patch clamp recordings and neuronal reconstructions. Working memory (WM) impairment, neuronal hyperexcitability, and spine loss began in middle age. There was no significant relationship between neuronal properties and WM performance. Middle-aged subjects given curcumin exhibited better WM performance and less neuronal excitability compared to control subjects. These findings suggest that the appropriate time frame for intervention for age-related cognitive changes is early middle age, and points to the efficacy of curcumin in delaying WM decline. Because there was no relationship between excitability and behavior, the effects of curcumin on these measures appear to be independent.

Keywords

working memory; *in vitro* slice; electrophysiology; morphology; Delayed Recognition Span Task

[*]Corresponding Author: jluebke@bu.edu; 617-358-9595; X-317 650 Albany St., Boston MA 02118 USA.

Author Contributions

Wayne Chang, Christina Weaver and Jennifer Luebke: Conceptualization, Methodology, Investigation, Data curation and analysis, Writing- Original, Reviewing and Editing. **Tara Moore and Maria Medalla**: Investigation, Data curation and analysis.

Declaration of interest: none

1. Introduction

A significant proportion of humans and non-human primates exhibit declines in working memory during normal aging (Bartus et al., 1979; Herndon et al., 1997; Moore et al., 2006; Murman, 2015; Salthouse, 2012). While the neural underpinnings of these age-related changes have yet to be fully elucidated, we and others have described sublethal changes to neurons, glial cells, and vascular elements during aging in the rhesus monkey brain that likely lead to dysfunction at the network, regional and behavioral levels (Hof and Morrison, 2004; Luebke et al., 2010; Morrison and Baxter, 2012; Peters and Kemper, 2012; Rozycka and Liguz-Lecznar, 2017; Xekardaki et al., 2015). For example, layer 3 (L3) pyramidal neurons in area 46 of the Lateral Prefrontal Cortex (LPFC)—a key mediator of working memory (Jacobsen, 1935; Lara and Wallis, 2015)—exhibit age-related structural changes including significant reductions in dendritic spine densities and in asymmetric and symmetric synapses, together with extensive myelin dystrophy and degeneration (Peters et al., 2008; Peters, 2009). At the functional level, LPFC pyramidal neurons exhibit action potential hyperexcitability and alterations in both inhibitory and excitatory synaptic activity *in vitro* with age (Chang et al., 2005; Luebke et al., 2004). These L3 pyramidal neurons form extensive recurrent intralaminar connections within the LPFC (Kritzer and Goldman-Rakic, 1995), and the excitatory activity generated by these horizontal connections has been identified as key to the maintenance of relevant information during working memory (Bastos et al., 2018). Thus, the observed structural and functional alterations to LPFC neurons with age likely lead to aberrant processing of information within local and long-range LPFC circuits and consequently to age-related deficits in frontal lobe functions including working memory.

While effects of aging on functional and structural properties of L3 pyramidal neurons in the LPFC of rhesus monkeys have been demonstrated through categorical comparisons between neurons of young and aged animals (Chang et al., 2005; Coskren et al., 2015; Ibañez et al., 2020; Luebke et al., 2004), little is known about the cause or the detailed temporal trajectory during aging of these multifaceted alterations. Because the onset of cognitive decline occurs during middle age in both humans and nonhuman primates (Moore et al., 2006; Salthouse, 2009), as does the initial breakdown of frontal white matter (Bowley et al., 2010), alterations to neuronal properties likely manifest at a similar time point. Closer examination of subjects across the adult lifespan and including middle-aged subjects as performed in the present study provides a more complete understanding of how age-related changes progress in the primate brain and aids in the identification of the underlying cause of cognitive changes that negatively affect the activities of daily life.

Recent studies have focused on the role of oxidative stress and inflammation on the exacerbation of age-related pathology, both in the peripheral and the central nervous systems. Within the brain, alterations in the balance between the concentrations of reactive oxygen and nitrogen species and the cellular defense mechanisms results in a build-up of oxidative stress with increasing age (Holmström and Finkel, 2014; Kawagishi and Finkel, 2014). Elevated oxidative stress and inflammation in the aging brain lead to neuronal dysfunction and ultimately to disruption of neuronal networks that mediate behavioral function (Wang and Michaelis, 2010), but the mechanisms and relationships between these

processes remain unclear. Due to its strong antioxidant and anti-inflammatory properties, curcumin, a major polyphenolic component of turmeric (Menon and Sudheer, 2007), has been widely tested as a potential nutraceutical supplement to slow or reverse detrimental effects of aging. In humans and in rodent models, curcumin has been shown to delay the process of senescence including the onset or progression of age-related changes in cognitive functions such as spatial working memory (Cox et al., 2015; Grabowska et al., 2017; Nam et al., 2014; Rainey-Smith et al., 2016; Salvioli et al., 2007; Sikora et al., 2010b, 2010a). Further, curcumin has been demonstrated to exert numerous neuroprotective effects (Borre et al., 2014; Tegenge et al., 2014; Williams et al., 2014; Yang et al., 2014). While most studies have been conducted in rodents, we have recently demonstrated the efficacy of chronic dietary curcumin administration as a treatment to improve spatial working memory in a cohort of middle-aged nonhuman primates (Moore et al., 2017). In humans, clinical studies on curcumin as a potential treatment for both normal aging and mild or moderate Alzheimer's Disease have yielded mixed results (Sarker and Franks, 2018). A better understanding of the influence of dietary curcumin on neurons *per se* is necessary to evaluate its efficacy as a nutraceutical supplement to treat age-related cognitive decline related to neuronal changes in specific brain areas.

Here we elucidated the temporal progression of age-related changes to working memory performance and the morphological and functional properties of L3 pyramidal neurons in the LPFC of the same rhesus monkeys across the adult lifespan—between 5.5 and 29.5 years of age. Further, we assessed the ability of chronic dietary curcumin to slow or reverse age-related changes to behavior and neuronal properties in the LPFC of middle-aged rhesus monkeys. The data confirm that deficits in working memory begin in early-middle age, and reveal that significant changes to the structure and function of neurons occur at a similar time point during the aging process. Furthermore middle-aged subjects given dietary curcumin exhibited better working memory performance and less excitability of neurons compared to control middle-aged and aged subjects.

2. Materials and Methods

2.1 Experimental Subjects

Published archived (Chang et al., 2005; Coskren et al., 2015; Ibañez et al., 2020; Moore et al., 2017) and new data from rhesus monkeys (*Macaca mulatta*), 5.5 to 29.5 years of age (y.o.), contributed to this study. Age was treated as a continuous variable for all analyses with the exception of the Sholl and MANOVA (see statistical analysis section below). For categorical comparisons, ages were rounded to the nearest integer, and monkeys were divided into three age groups: young (6–12y.o.; 9 males, 4 females); middle-aged (13–20y.o.; 4 males, 14 females); and aged (21–28y.o.; 9 males, 5 females); these animals were a part of a larger study of normal aging in nonhuman primates, conducted over the course of 14 years. The cutoffs for age groups were determined based on a suggested ratio of 1:3 between rhesus monkey and human years of age (Tigges et al., 1988); middle age, commonly defined as being between the ages of 40 and 60 in humans, corresponds to the age range of 13–20 years of age in rhesus monkeys. A separate cohort of 7 middle-aged animals (3 males, 4 females) received a daily oral dose of 500mg of dietary

curcumin treatment for ~2 years, as described (Moore et al., 2017). The curcumin was Longvida® Optimized curcumin that was manufactured and supplied by Verdure Sciences (Noblesville, IN). All but six animals in this study underwent cognitive testing prior to sacrifice, and curcumin-treated animals, along with a subset of middle-aged controls, were subjected to an additional round of testing ~8 weeks after the initial round. Data from 39 animals was used for electrophysiological experiments, 24 subjects contributed data for dendritic morphological studies, and 20 subjects contributed to spine analyses. Monkeys were obtained from various National Primate Research Centers and private vendors and had known birth dates and complete health records. Before entering the study, monkeys received medical examinations that included serum chemistry, hematology, urine analysis and fecal analysis. In addition, all monkeys underwent magnetic resonance imaging to ensure there was no occult neurological damage. Results of the medical exams and MRIs revealed that all monkeys were healthy at the time they were entered into the study. While on study, monkeys were individually housed in colony rooms where they were in constant auditory and visual range of other monkeys in the Animal Science Center (ASC) of Boston University Medical Campus. This facility is fully AAALAC approved and animal maintenance and research were conducted in accordance with the guidelines of the National Institutes of Health and the Institute of Laboratory Animal Resources Guide for the Care and Use of Laboratory Animals. All procedures were approved by the Boston University Institutional Animal Care and Use Committee. Diet consisted of Purina Monkey Chow (Purina Mills Inc, St. Louis, MO) supplemented by fruit with feeding taking place once per day, immediately following behavioral testing. All monkeys were fed 12–20 biscuits per day based on their weight. During testing, small pieces of fruit or candy were used as rewards. Water was available continuously. The monkeys were housed under a 12-hour light/dark cycle with cycle changes occurring in a graded fashion over the course of an hour. Enrichment procedures included provision of dietary items (e.g. frozen yogurt and fruit) and devices (e.g. chew toys, foraging devices and audio and visual stimulation) all of which meet or exceed USDA guidelines. The enrichment procedures have been in place in the Moore laboratory for over 10 years and are employed consistently with all monkeys.

2.2 Behavioral Assessment

Delayed Recognition Span Task, both spatial (DRST-Spatial) and object (DRST-object) conditions, were performed to assess working memory function of the animals, as previously described in (Killiany et al., 2000; Moore et al., 2017). Both conditions were performed using a board containing 18 wells (3.5cm wide, 0.5cm deep) arranged in a 3 × 6 matrix. In the initialization of a trial, one well was baited with a food reward, and covered with a stimulus. The subject then removed the stimulus to retrieve the reward, after which the door was lowered. The first stimulus was then placed over an unbaited well, and a new stimulus added to a baited well. The door was raised after 10s, and the subject was required to identify the newly-presented stimulus in order to obtain the reward. Each successive correct identification was followed by the addition of a new stimulus until an error was made. The number of correctly-identified new stimuli was then recorded as the recognition span score for that trial. In each round of testing, 100 trials were administered over 20 consecutive days (5 trials per day). For DRST-Spatial, identical brown discs (6cm in diameter) were used as stimuli, and discs were returned to their original location after each correct identification.

On the other hand, for the object condition, stimuli were drawn from a pool of random junk objects, and within each trial, the position of previously-presented objects were shifted in a pseudorandom fashion to ensure that the subject is identifying the novel object based on visual, and not spatial, cues. Because the interval between the date of behavioral testing and the date of animal euthanasia and brain perfusion varied between cohorts, the age at testing, rather than the age at perfusion, was used for the behavioral (but not single neuron) analyses.

2.3 Preparation of acute brain slices

Monkeys were euthanized as described in our previous publications (Ibañez et al., 2020; Medalla et al., 2017; Medalla and Luebke, 2015). Briefly, after perfusion with ice-cold Krebs-Henseleit buffer (concentrations in mM: 6.4 Na_2HPO_4, 1.4 Na_2PO_4, 137 NaCl, 2.7 KCl, 5 glucose, 0.3 $CaCl_2$, 1 $MgCl_2$, pH 7.4), a block of tissue (~1cm^3) was removed from the left lateral prefrontal cortex (area 46), and transferred into ice-cold oxygenated (95% O_2 / 5% CO_2) Ringer's solution (concentrations in mM: 26 $NaHCO_3$, 124 NaCl, 2 KCl, 3KH_2PO_4, 10 glucose, 1.3 $MgCl_2$, pH 7.4; Sigma-Aldrich) and sectioned into 300μm-thick coronal slices on a vibrating microtome. Slices were immediately placed into room temperature oxygenated Ringer's solution and equilibrated for a minimum of one hour before recording.

2.4 Whole-cell patch clamp recordings

Individual slices were placed in submersion-type recording chambers (Warner Instruments) mounted on Nikon E600 infrared-differential interference contrast (IR-DIC) microscopes. Throughout the duration of the recordings, slices were continuously superfused with room temperature oxygenated Ringer's solution (at a flow rate of 2–2.5ml/min). Standard tight-seal whole-cell patch clamp recordings were performed on visually-identified L3 pyramidal neurons, as described previously (Ibañez et al., 2020; Medalla et al., 2017; Medalla and Luebke, 2015). Electrodes were fabricated on a Flaming/Brown-type micropipette puller (model P-87, Sutter Instrument), and filled with a potassium methane sulfonate (KMS)-based internal solution (concentrations in mM: 122 KCH_3SO_3, 2 $MgCl_2$, 5 EGTA, 10 NaHEPES, 0.5% biocytin, pH 7.4), with resistances of 3–7MΩ in Ringer's external solution. Data were acquired with EPC-9 or EPC-10 amplifiers controlled by PatchMaster acquisition software (HEKA Elektronik). Access resistance was monitored and maintained throughout the experiments, and signals were low pass-filtered at 10kHz.

2.5 Assessment of electrophysiological properties

Current clamp protocols were implemented as previously described (Gilman et al., 2017; Medalla et al., 2017; Medalla and Luebke, 2015). Briefly, passive neuronal properties (resting membrane potential V_r, input resistance R_n and membrane time constant tau) were assessed with a series of 200ms hyperpolarizing and depolarizing current steps. R_n and V_r were extracted as the slope and intercept of the best-fit line of the voltage-current relationship, respectively. Tau was calculated by fitting a single-exponential curve to the neuronal response to a −10pA hyperpolarizing current step. Single action potential (AP) properties (threshold, amplitude, rise time, fall time, half-max duration) were measured from the second –in a train of three or more APs— elicited by the smallest depolarizing current step in the protocols. Rheobase, the minimum amount of current required to elicit an AP,

was assessed with a 10s depolarizing current ramp. Firing frequencies were calculated from a series of 2s hyperpolarizing and depolarizing current steps (−220–280pA, increments of 50pA). The electrophysiological traces of neurons that meet to inclusion criteria (V_r <= −55mV, stable AP overshoot, and repetitive firing responses) were imported into MATLAB (MathWorks, Inc) for semi-automated analysis of neuronal properties.

2.6 Processing of biocytin-filled neurons

Following recording, slices were immediately placed in 4% paraformaldehyde (in 0.1M PBS) for 48 hrs. at 4°C for fixation. After rinsing, slices were incubated in 1% Triton X (in 0.1M PBS), and transferred to streptavidin-Alexa 488 (1:500 in 0.1M PBS; Invitrogen) for 48hrs at 4°C. Subsequently, slices were rinsed in 0.1M PBS and stored in anti-freeze solution (30% glycerol, 30% ethylene glycol in 0.05M phosphate buffer) at −20°C.

2.7 Confocal microscopy

Slices containing neurons that met the inclusion criteria (lack of dendritic varicosities, completeness of apical dendrites and high signal-to-noise ratio) were rinsed in 0.1M PBS, then mounted and coverslipped in ProLong Antifade mounting medium (Invitrogen). Scans were acquired with a Leica SPE confocal microscope (Leica Microsystems). For dendritic analysis, serial optical sections spanning the entirety of neurons were imaged at 0.3 × 0.3 × 0.3μm per voxel (40×/1.3NA oil-immersion objective, 488nm excitation wavelength). For spine analysis, three fields of view (FOVs) were selected for each neuron: one containing the distal-most part of an apical dendrite, one containing the apical dendritic trunk, and one containing the middle portion of a basal dendrite. Serial optical sections were imaged for each FOV at 0.04 × 0.04 × 0.2μm per voxel (63×/1.4NA oil-immersion objective, 488nm excitation wavelength). All image stacks were imported to AutoQuant Software (Media Cybernetics) for deconvolution, and dendritic image stacks were aligned and merged using Volume Integration and Alignment System (VIAS) software (Rodriguez et al., 2003) to generate a single image stack for each neuron.

2.8 Morphometric reconstruction and analysis

Measurements of dendritic span (soma-to-apical tip, vertical and horizontal extent of apical tuft, apical obliques and basal dendrites) were taken using the measurement function in Fiji, calibrated to pixel dimensions of confocal images. Image stacks were imported into NeuronStudio software (Rodriguez et al., 2006), and dendritic arbors were semi-automatically reconstructed in their entirety. Independent analysis of dendritic length, branch points, and arbor complexity were employed for apical and basal dendritic arbors separately. To account for differences in depth of somata between neurons, apical dendritic properties were normalized by the soma-to-pia distance of each neuron. For the Sholl analyses of apical dendrites, the radii of concentric rings placed at increasing distances from the soma were normalized by the soma-to-pia distance of each neuron, amounting to 10 total rings ranging from 10–100% of the soma-to-pia distance. The resulting dendritic length and number of branch points within each ring were then normalized by the bin width. Sholl analyses for basal dendrites of all neurons were conducted with spheres of 20μm increments. For the assessment of spine density, all spines along the reconstructed dendrite within each FOV were identified and marked, and the density within each FOV was calculated.

2.9 Statistical analysis

All analyses were performed in RStudio 1.4.1717, except the one-way multivariate ANOVA (MANOVA) analysis performed in MATLAB 2020a (MathWorks, Inc.). Age was treated as a continuous variable in all analyses except for the Sholl dendritic data and the MANOVA, in which subjects were classified categorically into young, middle-aged and aged groups (see experimental subjects, above). For behavioral data, standard linear regressions were used to measure differences in performance with aging, and difference in percent-change in performance between curcumin treated and control middle-aged animals. Percent-change in behavioral performance was calculated as follows: 100*(round 2 span – round 1 span) / round 1 span. For neuronal properties, in which multiple neurons per subject were collected, generalized linear mixed-effects models (GLMMs) were used with subject treated as a random effect blocking (nesting) factor (Aarts et al., 2014; Darian-Smith et al., 2013; Grafen and Hails, 2002). Variance explained by fixed factors was quantified by marginal R^2; variance explained by the whole model including random effects was quantified by conditional R^2. For the physiological data monkeys with at least five recordings were included, with outlier analysis performed on resting membrane potential, input resistance, and rheobase for each age group. Data falling more than 1.5 interquartile range above the upper quartile or below the lower quartile of these variables were omitted as outliers. Firing rates in response to current injections 180 pA and above were included together as a multiple regression of firing rates versus age and injection magnitude. Visual inspection identified no outliers for DRST-Spatial span, dendritic morphology, or spine density data versus age. Two young outliers for the DRST-Object span were not omitted, as their inclusion did not change the outcome of tests. In analyses comparing curcumin treatment with age-matched controls, curcumin treatment was included as a separate regression factor (an indicator variable, as either 0 or 1). Sholl data comparing dendritic complexity in the three age groups was analyzed using two-way repeated measures ANOVA, including subject as a random effect and Sholl rings as the repeated measure. To focus analyses on the most relevant regions, the Sholl data were examined to identify a small number of consecutive rings where differences among age groups seemed most likely (apical arbors: rings from 80 to 100% of the normalized soma-to-pial distance; basal arbors: rings from 140 to 180μm). Tukey-adjusted comparison of estimated marginal means was used to conduct post-hoc analyses. In analyses considering relationships between behavioral responses to other variables, measurements of individual neurons were first averaged by subject. MANOVA was used to examine the relative similarities and dissimilarities between age groups based on neuronal properties with significant group differences, as described (Medalla, Chang et al., 2020). Neuronal properties were separated into two categories and converted to standard normal units. Outcome measures included in each category are as follows: *Electrophysiology:* R_n, rheobase, and firing frequency at 280 pA current injection (firing frequencies at other injections were highly correlated with 280 pA data and omitted); *Spine Density:* distal apical and basal spine density (mid-apical density was highly correlated with these and omitted). Significant dimensions of the means were evaluated with the Wilks' lambda test statistic, built-in to the manova1 function in MATLAB and pairwise Mahalanobis distance analyses. In all cases, differences were considered significant when $p < 0.05$.

3. Results

3.1 Performance on the Delayed Recognition Span Task (DRST)

We assessed age-related changes in working memory performance using two conditions of the Delayed Recognition Span Task—spatial (DRST-Spatial) and object (DRST-Object)—and linear regression of data from all monkeys. For DRST-Spatial, but not -Object, there was a significant decrease in performance with age (regression, Spatial = −0.027*Age + 2.78, R^2 = 0.097, $F_{(1,37)}$ = 5.09, p=0.030, Fig. 1A, left; Object: $F_{(1,37)}$ = 3.07, p = 0.088, Fig. 1B, left). This was consistent with previous studies (Herndon et al., 1997; Ibañez et al., 2020) in which young subjects performed significantly better than aged subjects, and confirmed that deficits in working memory begin in early middle age, with subjects having a span of less than 2.2 on -Spatial and 2.39 on -Object classified as impaired relative to young subjects. Importantly, and as with previous studies (Moss et al., 2007; Plagenhoef et al., 2021), a significant proportion of aging monkeys, including those among the oldest did not show impairment relative to the young subjects and thus can be considered unimpaired or ―successful‖ agers. To evaluate the effect of curcumin treatment on DRST performance, a subset of animals (3 male and 4 female curcumin-treated subjects, 1 male and 10 female non-treated control subjects) underwent one additional round of testing ~8 weeks after the initial round. Behavioral measures were compared using the percent change in performance from the first to the second round. There were greater improvements in performance over sequential rounds of DRST-Spatial testing in monkeys treated with dietary curcumin compared to age-matched controls who were not given curcumin (Spatial = 18.55*Curcumin + 4.97, $F_{(1,16)}$ = 9.87, p = 0.006, Fig. 1A, right), consistent with our previous work (Moore et al., 2017). The curcumin-treated animals also showed significantly greater improvements in DRST-Object performance (Object = 9.98*Curcumin - 8.07, $F_{(1,16)}$ = 5.213, p = 0.036, Fig 1B, right). Together, these data illustrate that age-related decline in working memory performance begins in early-middle age, and that chronic dietary curcumin administration improves both spatial- and object-working memory in middle-aged animals.

3.2 Electrophysiological properties of L3 pyramidal neurons

A comparison of passive membrane properties revealed no age-related change in resting membrane potential or membrane time constant (V_r, p = 0.64; tau, p = 0.54; not shown). Input resistance increased significantly from the onset of early middle age (age 13) through age 25 (R_n=8.52*Age+13.1 MΩ, marginal R^2 = 0.09, conditional R^2 = 0.22, p =0.008, Fig. 2A, left, middle), but did not follow one linear change consistently across all ages (R_n, p=0.058). Rheobase decreased significantly with aging (Rheo = −1.70*Age + 121.5 mV/ms, marginal R^2 = 0.06, conditional R^2 = 0.32, p = 0.022; Fig. 2B, left, middle). Analyses of single AP properties revealed no differences with aging in amplitude, duration, rise time or fall time (p = 0.26, p = 0.73, p = 0.38, and p = 0.11 respectively; not shown). AP firing in response to 2s current injections of 130 pA and above increased significantly with age (multiple regression, FR = 0.10*inj + 0.16*Age – 11.6 Hz, marginal R^2 = 0.46, conditional R^2 = 0.51, p = 0.011; Fig. 2C left, middle). Those physiological properties that were unchanged with aging were also similar in animals treated with dietary curcumin versus age-matched control animals (tau, p = 0.59; Vr, p = 0.13; AP amp, p = 0.059; all other single AP properties, p ≥ 0.27). There was a significant increase in R_n and decrease in rheobase

with aging in this subset of control and curcumin treated animals (R_n = 14.0*Age – 88.5 MΩ, marginal R^2 = 0.06, conditional R^2 = 0.12, p=0.005; Fig. 2A, right; Rheo = −12.5*Age + 340.2 mV/ms, marginal R^2 = 0.16, conditional R^2 = 0.33, p = 0.002; Fig. 2B, right), but adding curcumin treatment as a factor in the analyses had no significant effect (p = 0.54 and p = 0.92 respectively). In contrast, curcumin treatment had a significant subtractive effect on AP firing rates in response to current steps above 130 pA (multiple regression, FR = 0.047*inj + 1.62*Age - 2.22*Curcumin - 25.3 Hz, marginal R^2 = 0.29, conditional R^2 = 0.33, p=0.011; Fig. 2C, right). We averaged each physiological variable within each subject, then performed linear regressions versus DRST-Spatial or DRST-Object performance; these analyses revealed no significant correlation (p ≥ 0.25; not shown). Overall the physiological results confirmed the previously reported effect of age on the physiology of L3 pyramidal neurons in the LPFC, namely hyperexcitability, manifested in both passive (R_n) and active (rheobase, FR) properties (Chang et al., 2005; Ibañez et al., 2020). The present study extends previous work by showing that the onset of changes occurs in middle age, and that curcumin treatment is associated with lower firing rates in middle-aged and aged animals.

3.3 Morphological properties of L3 pyramidal neurons

The morphology of individual L3 pyramidal neurons was characterized both at the level of the complete dendritic arbor and at the level of spines on localized dendritic compartments. There was a significant decrease in total length of the dendritic arbor with aging (ApicalLength = −11.8*Age + 1100.8%, marginal R^2 = 0.10, conditional R^2 = 0.10, p = 0.046; Fig. 3), but no other significant changes with aging in overall dendritic morphology, including average measures of dendritic span, length, and complexity (p ≥ 0.79; Fig. 3). A more detailed examination of dendritic length and branch points using Sholl analysis (Sholl, 1953) revealed no differences among age groups for either apical or basal arbors (repeated measures ANOVA, p ≥ 0.14; not shown). Dendritic morphological features did not differ significantly between neurons from curcumin treated animals and those from age-matched controls (p > 0.68; dendritic length as an example, Fig. 3B, right). Spine density was quantified across three different dendritic locations on each neuron: distal apical, mid-apical, and basal (Fig. 4). The overall spine density in mid-apical dendrites was about twice that in the distal apical and basal compartments, but was also highly correlated with those densities (r = 0.76 and r = 0.77 between mid-apical and basal, and mid-apical and distal respectively). The rate of age-related spine loss was greatest in mid-apical dendrites (MidDensity = −0.073*Age + 2.65#/μm, marginal R^2 = 0.38, conditional R^2 = 0.51, p = 0.002), more than twice the rate of spine loss in distal apical and basal dendrites (Distal = −0.031*Age + 1.27#/μm, marginal R^2 = 0.44, conditional R^2 = 0.50, p < 0.0001; Basal = −0.033*Age + 1.36#/μm, marginal R^2 = 0.46, conditional R^2 = 0.63, p = 0.001; Fig. 4, middle panels). After using Z-scores to normalize each quantity, regressions revealed that relative rates of spine loss in all three compartments were similar (NormMid = −0.085*Age + 1.42; NormDistal = −0.096*Age + 1.64; NormBasal = −0.095*Age + 1.58). These were much higher than the relative rates of change in apical length, rheobase, or firing rates (NormApicLen = −0.046*Age + 0.795; NormRheo = −0.04*Age + 0.66; NormFR = 0.02*Age + 0.67*NormInj – 0.34). Spine density of neurons from animals that received dietary curcumin did not differ from that of neurons from the control group, in any compartment (p>0.15; Fig. 4, right panels). As with the physiological data, we averaged

each morphological variable within each subject, then performed linear regressions versus DRST-Spatial or DRST-Object performance, and found no significant correlation ($p \geq 0.25$; not shown). Such extensive reductions in spine density are well-established to occur in pyramidal neurons from aged rhesus monkeys (Cupp and Uemura, 1980; Dickstein et al., 2013; Duan et al., 2003; Kabaso et al., 2009). Our data extend these previous studies by demonstrating that spine loss begins in early middle age.

3.4 Multivariate analysis of variance of electrophysiological and spine data

To elucidate the relationship between neuronal properties that varied significantly during aging and the temporal progression of such changes, multivariate analysis of variance (MANOVA) was performed for electrophysiological properties (R_n, rheobase, FR) and spine density. The three age groups were used as predictor variables, and outcome measures that significantly differed with aging as response variables (Fig. 5). This analysis on the electrophysiological data revealed one significant dimension that separated the aged neurons from neurons of the younger age groups ($p = 0.012$; Fig. 5A). The MANOVA revealed two significant dimensions that separated the groups based on spine density- the first separating aged neurons from neurons from the younger two groups, and the second separating young and middle-aged neurons ($p = 0.002, 0.009$; Fig. 5B). The MANOVA results revealed greater temporal progressions of spine density changes than those of physiological properties: the second dimension separating young and middle aged was significant for spine density but not electrophysiology variables. Also, among components of the first-order canonical vectors that distinguished aged data from the younger age groups, physiological variable weights were similar in magnitude to each other (Fig. 5C), but smaller than the basal spine density weight. Distal spine density contributed very little in distinguishing aged monkeys from other groups, but was the main factor distinguishing young versus middle-aged monkeys (c2; Fig. 5D).

4. Discussion

Here we examined the age-related changes to the functional and structural properties of L3 pyramidal neurons in the LPFC and performance on the DRST by rhesus monkeys across the adult lifespan. We also assessed the ability of dietary curcumin to ameliorate changes to neurons and to behavior in middle-aged animals. We replicated previous reports of changes to neuronal properties and working memory function in aged animals (Chang et al., 2005; Coskren et al., 2015; Herndon et al., 1997; Ibañez et al., 2020; Kabaso et al., 2009), and demonstrated that the onset of the most significant changes—hyperexcitability, spine loss and working memory impairment—occurs relatively early in the aging process during middle age. Furthermore, we showed that dietary curcumin improves working memory performance and also prevents the age-associated increase in evoked firing rates of neurons *in vitro*, but that working memory performance and firing rates of neurons in the same subjects were not significantly correlated.

4.1 Age-related impairments in working memory begin in middle age

Age-related cognitive decline in a significant proportion of humans and nonhuman primates has been well documented (Bartus et al., 1979; Herndon et al., 1997; Moore et al., 2005,

2003, 2006; Murman, 2015; Salthouse, 2012; Wang et al., 2011). Higher-order cognitive functions, such as executive function and working memory mediated by the LPFC are especially vulnerable compared to sensory functions such as visual discrimination (Bartus et al., 1979; Moore et al., 2005, 2006; Rapp, 1990; Wang et al., 2011). Impairment on numerous behavioral tests of executive function in rhesus monkeys—including those for recognition memory, working memory, and reversal learning—has long been established (Herndon et al., 1997; Lacreuse et al., 2005). Furthermore, we have previously demonstrated that in rhesus monkeys, the onset of age-related working memory impairment, as assessed with the Category Set Shifting Task, begins in middle age (Moore et al., 2006). On this task, middle-aged and aged animals demonstrated impaired abstraction, set-shifting, and working memory and showed a greater tendency to perseverate. In agreement with these previous reports, in the present study we demonstrate a continuous decline of spatial working memory over the aging process—as assessed with the spatial condition of DRST—beginning in early middle age. In summary, there is growing evidence that declines in LPFC mediated functions, such as working memory, abstraction, set shifting and perseveration begin in early middle age, which is thus an appropriate age for therapeutic interventions such as dietary curcumin. It is important to note that many cross sectional and longitudinal studies of aging have demonstrated that some middle-aged and aged subjects are ―successful agers‖ in that their working memory performance does not differ from young subjects, while others are ―unsuccessful agers‖ that exhibit reduced working memory abilities (Moss et al., 2007; Plagenhoef et al., 2021); this was clearly the case in the present study where several middle-aged and aged subjects were successful agers. The mechanisms of age-related declines in working memory function in some but not all monkeys (or humans) are currently unknown, but likely include an array of sublethal changes to neurons and circuits in the LPFC and associated cortical structures, such as white matter, dendritic spine and synapse loss leading to alterations in the timing of neuronal signaling required for working memory (review: Luebke et al., 2010)

4.2 Changes to electrophysiological properties of L3 pyramidal neurons begin in middle age

Consistent with our previous finding of elevated evoked action potential firing rates in L3 pyramidal neurons in the aged monkey LPFC (Chang et al., 2005; Coskren et al., 2015; Ibañez et al., 2020; Kabaso et al., 2009), the present results demonstrate several signs of increased neuronal excitability across the adult lifespan, including significantly elevated input resistance and AP firing frequency, as well as decreased rheobase. Importantly, the present analyses include neurons from middle-aged animals (13–20 y.o.), which revealed the early onset of these age-related physiological changes. While increases in action potential firing rate of pyramidal neurons recorded *in vitro* are well-established to occur during aging, and likely have important consequences at the network level, the underlying mechanism(s) of such change is currently unknown. One plausible mechanism is myelin damage within the frontal white matter, which begins in middle age (Bowley et al., 2010), as Hamada and Kole (2015) have illustrated that damage to myelin induces hyperexcitability of L5 gray matter neurons. While L3 pyramidal neurons do not have long range projections as extensive as L5 neurons, they do give rise to local, recurrent, and callosal projections that may be impacted significantly by loss of myelin. Indeed, L3 pyramidal neurons in the LPFC possess

dense local connectivity that facilitates persistent activity during the execution of working memory tasks. Notably, a previous study using *in vivo* extracellular recordings of pyramidal neurons in monkey LPFC during the execution of a spatial working memory task revealed that while baseline firing rates were unchanged with age, a subset of delay-period active neurons showed reduced firing rates during the delay period of the task in middle-aged and aged subjects compared to young (Wang et al., 2011). This report of no baseline change in firing rate, together with delay-specific reduction of firing rates seems initially at odds with our demonstration of increased firing rates of pyramidal neurons in LPFC slices. How might this apparent discrepancy be reconciled? First, unlike the *in vivo* studies, the *in vitro* studies undertaken here cannot discriminate between task-specific neuronal populations but rather assessed a heterogeneous population of neurons with evoked step depolarizations. This was underscored by the finding that there was no significant relationship between firing rate *in vitro* and DRST performance scores in the cohorts studied here. It is important to bear in mind that the dramatic loss of spines together with well-established myelin dystrophy in aging likely underlie a loss of the recurrent excitation that is critical for the task-phase specific firing rate increases. Loss of recurrent excitation *in vivo* may be extensive enough to overcome intrinsic hyperexcitability of pyramidal neurons observed in the deafferented slice preparation.

4.3 Changes to the morphology of L3 pyramidal neurons begin in middle age

There was a modest reduction in the total dendritic length of the apical dendrites of L3 pyramidal neurons with aging, while all other features of both apical and basal dendritic topology such as number of dendritic branch points and vertical and horizontal dendritic extent did not change. By contrast to the dendritic arbor, there were dramatic age-related reductions of dendritic spines in the distal apical, mid-apical and basal dendritic compartments. Thus the present study recapitulates previous reports by our group and others of significantly reduced spine densities in both apical and basal dendrites of cortical neurons in aged humans and nonhuman primates (Benavides-Piccione et al., 2013; Cupp and Uemura, 1980; Dickstein et al., 2013; Duan et al., 2003; Kabaso et al., 2009; Page et al., 2002). Interestingly, with higher spine densities in mid-apical dendrites overall, spine loss in mid-apical dendrites occurs at a more rapid rate than in the distal-apical and basal compartments; however, the relative rates of spine loss in all compartments were similar. Dendritic spines are major sites of excitatory synapses, and consistent with the present findings, Peters et al. (2008) reported that the density of excitatory synapses in L2/3 of the LPFC are significantly negatively correlated with age over the adult lifespan of rhesus monkey. Furthermore, the loss of spines observed here and previously is in agreement with our report of decreased excitatory postsynaptic current frequency in L3 pyramidal neurons in LPFC slices from aged monkeys (Luebke et al., 2004). Reduced spine number and reduced excitatory synaptic drive are a likely mechanism underlying the reported reduction in persistent activity of these neurons recorded *in vivo* during the delay phase of working memory tasks by aged monkeys by Wang et al., (2011).

4.4 Differential time course of age-related changes to physiological and morphological neuronal properties

We performed MANOVA to better examine between-age group similarities based on neuronal properties that altered with age. The results reveal two distinct hierarchical structures that demonstrate the difference in temporal progression of changes in neuronal properties- reduction in spine density occurs at a more rapid rate compared to the elevation of excitability. This analysis also highlights the nuanced relationship between the location of a dendritic spine and its vulnerability to aged-related loss- distal-apical spine density best distinguished middle-aged from young neurons, whereas basal spine density was the dominating factor in the separation of aged neurons from those in the other age groups. This complemented a comparison of regression slopes of normalized electrophysiological and morphological variables. Distinct temporal progressions between physiological and morphological changes suggest separate underlying mechanisms of alterations with age. To better understand the interactions between the different types of properties—whether there is causality between them—further experiments will be required to obtain a larger sample of neurons from which functional and structural properties are both characterized.

4.5 Dietary curcumin ameliorates age-related changes to working memory and prevents neuronal hyperexcitability

Rhesus monkeys that received dietary curcumin exhibited significantly greater improvements in both spatial and object working memory performance over consecutive testing rounds, as assessed with DRST-Spatial and -Object tasks. This result is consistent with that of our previous study, in which the same effect was observed in an overlapping, but not identical, cohort of animals (Moore et al., 2017). At the neuronal level, curcumin administration reduced hyperexcitability of middle-aged and aged neurons. It would thus be tempting to speculate that the beneficial effect of curcumin on working memory performance may be due to its ability to reduce neuronal hyperexcitability by some unknown mechanism. However, while our previous studies did show significant relationships between firing rate and working memory performance—either U shaped (Chang et al., 2005) or negative linear (Ibañez et al., 2020)—there was no such significant relationship in the group of monkeys studied here. The reason for this difference in findings is likely due to the differences in the monkeys under study—while there was significant overlap, nearly a third of the subjects differed between the present study and Ibañez et al. (2020). These disparate findings highlight the heterogeneity of normal aging effects on the behavior and neuronal properties of individual monkeys. Nevertheless, it appears likely that the action of curcumin on firing rate and on working memory performance are independent effects.

Because no other physiological or morphological property measured in the present study was significantly altered with curcumin treatment, the reduction in firing rate is likely due to other underlying factors. Indeed, curcumin has been shown to reduce cytosolic calcium (Uğuz et al., 2016) and ensures the normal functioning of mitochondria (Bagheri et al., 2020; Rinwa and Kumar, 2012), which is not only required for sustained neuronal activity, but has also been recently demonstrated to be directly linked to neuronal firing rate (Styr et al., 2019). Alternatively, curcumin may exert an influence on neuronal excitability indirectly, through interactions with astrocytes and microglia (Eghbaliferiz et al., 2020; Ghasemi et al.,

2019), thereby enhancing glioprotective effects (Parada et al., 2015; Park et al., 2001). These various mechanisms are currently being assessed in ongoing studies in our laboratory.

The question arises as to the mechanism(s) by which curcumin ameliorates age-related working memory deficits, if not by reversing age-related changes to those structural and physiological properties of individual neurons assessed in the present study? As a powerful anti-oxidant and anti-inflammatory agent, curcumin has been demonstrated to exert many cellular effects that may be beneficial for cognitive function (reviews: Abrahams et al., 2019; Sarker and Franks, 2018; Voulgaropoulou et al., 2019). For example, curcumin enhances beneficial autophagy in the brain (review: Stacchiotti and Corsetti, 2020), increases mitochondrial energy production (Bagheri et al., 2020; Rinwa and Kumar, 2012), which may be required for persistent firing of neurons during the delay periods in working memory, and reduces cytosolic calcium (Uğuz et al., 2016) which may be protective of aging neurons in which calcium dyshomeostasis has been associated with cognitive deficits (Gant et al., 2015; Uryash et al., 2020). Although the action of curcumin on inflammation and oxidative stress on peripheral organ systems is well known (Hewlings and Kalman, 2017), the effect on the neuro-immune axis is not well understood. Indeed, while we have used a lipidated version of curcumin that has been shown to cross the blood brain barrier (Begum et al., 2008; Ma et al., 2013), it is not known whether curcumin was metabolized in the brains of monkeys in this cohort. Future work is needed to assess the dynamics of curcumin absorption and peripheral and central immune cell responses. Importantly, the age-related inflammatory and oxidative stress cascade in rhesus monkeys is not well understood. Previous work from our group has shown that myelin debris from age-related myelin damage can be the trigger for age-related brain inflammation in the white matter (Shobin et al., 2017). Thus, it is possible that in middle age, when myelin damage (Bowley et al., 2010) and neuronal hyperexcitability begin, inflammation and oxidative stress may still be low. It would be important to test the efficacy of curcumin in aged animals, where inflammation and oxidative stress are more severe, or in a longitudinal study design to assess if middle-age treatment with dietary curcumin can prevent future progression of age-related inflammation and neuronal dysfunction.

Acknowledgements:

The authors are grateful to Dr. Douglas Rosene for his assistance with preparation of in vitro slices. We also thank Verdure Sciences for their generous donation of the Longvida Curcumin and control vehicle used in this study. This work was funded by National Institute on Aging grants R01AG059028 (Luebke), R01-AG043478 and R01-AG043640 (Rosene)

References

Aarts E, Verhage M, Veenvliet J, Dolan C, van der Sluis S, 2014. A solution to dependency: using multilevel analysis to accommodate nested data. Nat. Neurosci 17, 491–496. 10.1038/NN.3648 [PubMed: 24671065]

Abrahams S, Haylett W, Johnson G, Carr J, Bardien S, 2019. Antioxidant effects of curcumin in models of neurodegeneration, aging, oxidative and nitrosative stress: A review. Neuroscience 406, 1–21. 10.1016/J.NEUROSCIENCE.2019.02.020 [PubMed: 30825584]

Bagheri H, Ghasemi F, Barreto G, Rafiee R, Sathyapalan T, Sahebkar A, 2020. Effects of curcumin on mitochondria in neurodegenerative diseases. Biofactors 46, 5–20. 10.1002/BIOF.1566 [PubMed: 31580521]

Bartus RT, Dean RL, Fleming DL, 1979. Aging in the rhesus monkey: Effects on visual discrimination learning and reversal learning. Journals Gerontol. 34, 209–219. 10.1093/geronj/34.2.209

Bastos AM, Loonis R, Kornblith S, Lundqvist M, Miller EK, 2018. Laminar recordings in frontal cortex suggest distinct layers for maintenance and control of working memory. Proc. Natl. Acad. Sci. U. S. A 115, 1117–1122. 10.1073/pnas.1710323115 [PubMed: 29339471]

Begum AN, Jones MR, Lim GP, Morihara T, Kim P, Heath DD, Rock CL, Pruitt MA, Yang F, Hudspeth B, Hu S, Faull KF, Teter B, Cole GM, Frautschy SA, 2008. Curcumin structure-function, bioavailability, and efficacy in models of neuroinflammation and Alzheimer's disease. J. Pharmacol. Exp. Ther 326, 196–208. 10.1124/jpet.108.137455 [PubMed: 18417733]

Benavides-Piccione R, Fernaud-Espinosa I, Robles V, Yuste R, Defelipe J, 2013. Age-based comparison of human dendritic spine structure using complete three-dimensional reconstructions. Cereb. Cortex 23, 1798–1810. 10.1093/cercor/bhs154 [PubMed: 22710613]

Borre YE, Panagaki T, Koelink PJ, Morgan ME, Hendriksen H, Garssen J, Kraneveld AD, Olivier B, Oosting RS, 2014. Neuroprotective and cognitive enhancing effects of a multi-targeted food intervention in an animal model of neurodegeneration and depression. Neuropharmacology 79, 738–749. 10.1016/j.neuropharm.2013.11.009 [PubMed: 24286859]

Bowley MP, Cabral H, Rosene DL, Peters A, 2010. Age changes in myelinated nerve fibers of the cingulate bundle and corpus callosum in the rhesus monkey. J. Comp. Neurol 518, 3046–3064. 10.1002/cne.22379 [PubMed: 20533359]

Chang YM, Rosene DL, Killiany RJ, Mangiamele LA, Luebke JI, 2005. Increased action potential firing rates of layer 2/3 pyramidal cells in the prefrontal cortex are significantly related to cognitive performance in aged monkeys. Cereb. Cortex 15, 409–418. 10.1093/cercor/bhh144 [PubMed: 15749985]

Coskren PJ, Luebke JI, Kabaso D, Wearne SL, Yadav A, Rumbell T, Hof PR, Weaver CM, 2015. Functional consequences of age-related morphologic changes to pyramidal neurons of the rhesus monkey prefrontal cortex. J. Comput. Neurosci 38, 263–283. 10.1007/s10827-014-0541-5 [PubMed: 25527184]

Cox K, Pipingas A, Scholey A, 2015. Investigation of the effects of solid lipid curcumin on cognition and mood in a healthy older population. J. Psychopharmacol 29, 642–651. 10.1177/0269881114552744 [PubMed: 25277322]

Cupp CJ, Uemura E, 1980. Age-related changes in prefrontal cortex of Macaca mulatta: Quantitative analysis of dendritic branching patterns. Exp. Neurol 69, 143–163. 10.1016/0014-4886(80)90150-8 [PubMed: 6771151]

Darian-Smith C, Lilak A, Alarcón C, 2013. Corticospinal sprouting occurs selectively following dorsal rhizotomy in the macaque monkey. J. Comp. Neurol 521, 2359–2372. 10.1002/CNE.23289 [PubMed: 23239125]

Dickstein DL, Weaver CM, Luebke JI, Hof PR, 2013. Dendritic spine changes associated with normal aging. Neuroscience. 10.1016/j.neuroscience.2012.09.077

Duan H, Wearne SL, Rocher AB, Macedo A, Morrison JH, Hof PR, 2003. Age-related dendritic and spine changes in corticocortically projecting neurons in macaque monkeys. Cereb. Cortex 13, 950–961. 10.1093/cercor/13.9.950 [PubMed: 12902394]

Eghbaliferiz S, Farhadi F, Barreto G, Majeed M, Sahebkar A, 2020. Effects of curcumin on neurological diseases: focus on astrocytes. Pharmacol. Rep 72, 769–782. 10.1007/S43440-020-00112-3 [PubMed: 32458309]

Gant J, Chen K, Kadish I, Blalock E, Thibault O, Porter N, Landfield P, 2015. Reversal of Aging-Related Neuronal Ca2+ Dysregulation and Cognitive Impairment by Delivery of a Transgene Encoding FK506-Binding Protein 12.6/1b to the Hippocampus. J. Neurosci 35, 10878–10887. 10.1523/JNEUROSCI.1248-15.2015 [PubMed: 26224869]

Ghasemi F, Bagheri H, Barreto G, Read M, Sahebkar A, 2019. Effects of Curcumin on Microglial Cells. Neurotox. Res 36, 12–26. 10.1007/S12640-019-00030-0 [PubMed: 30949950]

Gilman JP, Medalla M, Luebke JI, 2017. Area-Specific Features of Pyramidal Neurons-a Comparative Study in Mouse and Rhesus Monkey. Cereb. Cortex 27, 2078–2094. 10.1093/cercor/bhw062 [PubMed: 26965903]

Grabowska W, Sikora E, Bielak-Zmijewska A, 2017. Sirtuins, a promising target in slowing down the ageing process. Biogerontology 18, 447–476. 10.1007/S10522-017-9685-9 [PubMed: 28258519]

Grafen A, Hails R, 2002. Modern Statistics for the Life Sciences. Oxford University Press, New York, NY.

Hamada MS, Kole MHP, 2015. Myelin loss and axonal ion channel adaptations associated with gray matter neuronal hyperexcitability. J. Neurosci 35, 7272–7286. 10.1523/JNEUROSCI.4747-14.2015 [PubMed: 25948275]

Herndon JG, Moss MB, Rosene DL, Killiany RJ, 1997. Patterns of cognitive decline in aged rhesus monkeys. Behav. Brain Res 87, 25–34. 10.1016/S0166-4328(96)02256-5 [PubMed: 9331471]

Hewlings S, Kalman D, 2017. Curcumin: A Review of Its Effects on Human Health. Foods 6, 92. 10.3390/foods6100092

Hof PR, Morrison JH, 2004. The aging brain: Morphomolecular senescence of cortical circuits. Trends Neurosci 10.1016/j.tins.2004.07.013

Holmström KM, Finkel T, 2014. Cellular mechanisms and physiological consequences of redox-dependent signalling. Nat. Rev. Mol. Cell Biol 10.1038/nrm3801

Ibañez S, Luebke JI, Chang W, Draguljić D, Weaver CM, 2020. Network Models Predict That Pyramidal Neuron Hyperexcitability and Synapse Loss in the dlPFC Lead to Age-Related Spatial Working Memory Impairment in Rhesus Monkeys. Front. Comput. Neurosci 13. 10.3389/fncom.2019.00089

Jacobsen CF, 1935. Functions of frontal association area in primates. Arch. Neurol. Psychiatry 33, 558–569. 10.1001/archneurpsyc.1935.02250150108009

Kabaso D, Coskren PJ, Henry BI, Hof PR, Wearne SL, 2009. The electrotonic structure of pyramidal neurons contributing to prefrontal cortical circuits in macaque monkeys is significantly altered in aging. Cereb. Cortex 19, 2248–2268. 10.1093/cercor/bhn242 [PubMed: 19150923]

Kawagishi H, Finkel T, 2014. ROS and disease: Finding the right balance. Nat. Med 20, 711–713. 10.1038/nm.3625 [PubMed: 24999942]

Killiany RJ, Moss MB, Rosene DL, Herndon J, 2000. Recognition memory function in early senescent rhesus monkeys, Psychobiology.

Kritzer MF, Goldman-Rakic PS, 1995. Intrinsic circuit organization of the major layers and sublayers of the dorsolateral prefrontal cortex in the rhesus monkey. J. Comp. Neurol 359, 131–143. 10.1002/cne.903590109 [PubMed: 8557842]

Lacreuse A, Kim C, Rosene D, Killiany R, Moss M, Moore T, Chennareddi L, Herndon J, 2005. Sex, age, and training modulate spatial memory in the rhesus monkey (Macaca mulatta). Behav. Neurosci 119, 118–126. 10.1037/0735-7044.119.1.118 [PubMed: 15727518]

Lara AH, Wallis JD, 2015. The role of prefrontal cortex in working memory: A mini review. Front. Syst. Neurosci 10.3389/fnsys.2015.00173

Luebke J, Barbas H, Peters A, 2010. Effects of normal aging on prefrontal area 46 in the rhesus monkey. Brain Res. Rev 10.1016/j.brainresrev.2009.12.002

Luebke JI, Chang YM, Moore TL, Rosene DL, 2004. Normal aging results in decreased synaptic excitation and increased synaptic inhibition of layer 2/3 pyramidal cells in the monkey prefrontal cortex. Neuroscience 125, 277–288. 10.1016/j.neuroscience.2004.01.035 [PubMed: 15051166]

Ma QL, Zuo X, Yang F, Ubeda OJ, Gant DJ, Alaverdyan M, Teng E, Hu S, Chen PP, Maiti P, Teter B, Cole GM, Frautschy SA, 2013. Curcumin suppresses soluble Tau dinners and corrects molecular chaperone, synaptic, and behavioral deficits in aged human Tau transgenic mice. J. Biol. Chem 288, 4056–4065. 10.1074/jbc.M112.393751 [PubMed: 23264626]

Medalla M, Chang W, Calderazzo SM, Go V, Tsolias A, Goodliffe JW, Pathak D, de Alba D, Pessina M, Rosene DL, Buller B, Moore TL, 2020. Treatment with mesenchymal-derived extracellular vesicles reduces injury-related pathology in pyramidal neurons of monkey perilesional ventral premotor cortex. J. Neurosci 40, 3385–3407. 10.1523/JNEUROSCI.2226-19.2020 [PubMed: 32241837]

Medalla M, Gilman JP, Wang JY, Luebke JI, 2017. Strength and diversity of inhibitory signaling differentiates primate anterior cingulate from lateral prefrontal cortex. J. Neurosci 37, 4717–4734. 10.1523/JNEUROSCI.3757-16.2017 [PubMed: 28381592]

Medalla M, Luebke JI, 2015. Diversity of glutamatergic synaptic strength in lateral prefrontal versus primary visual cortices in the rhesus monkey. J. Neurosci 35, 112–127. 10.1523/JNEUROSCI.3426-14.2015 [PubMed: 25568107]

Menon VP, Sudheer AR, 2007. Antioxidant and anti-inflammatory properties of curcumin. Adv. Exp. Med. Biol 10.1007/978-0-387-46401-5_3

Moore T, Killiany R, Herndon J, Rosene D, Moss M, 2003. Impairment in abstraction and set shifting in aged rhesus monkeys. Neurobiol. Aging 24, 125–134. 10.1016/S0197-4580(02)00054-4 [PubMed: 12493558]

Moore T, Schettler S, Killiany R, Herndon J, Luebke J, Moss M, Rosene D, 2005. Cognitive impairment in aged rhesus monkeys associated with monoamine receptors in the prefrontal cortex. Behav. Brain Res 160, 208–221. 10.1016/J.BBR.2004.12.003 [PubMed: 15863218]

Moore TL, Bowley B, Shultz P, Calderazzo S, Shobin E, Killiany RJ, Rosene DL, Moss MB, 2017. Chronic curcumin treatment improves spatial working memory but not recognition memory in middle-aged rhesus monkeys. GeroScience 39, 571–584. 10.1007/s11357-017-9998-2 [PubMed: 29047012]

Moore TL, Killiany RJ, Herndon JG, Rosene DL, Moss MB file:///C:/Users/wayne/AppData/Local/Mendele. L.D. et al.-2006-E. system dysfunction occurs as early as middle-age in the rhesus monkey. pd., 2006. Executive system dysfunction occurs as early as middle-age in the rhesus monkey. Neurobiol. Aging 27, 1484–1493. 10.1016/j.neurobiolaging.2005.08.004 [PubMed: 16183172]

Morrison JH, Baxter MG, 2012. The ageing cortical synapse: Hallmarks and implications for cognitive decline. Nat. Rev. Neurosci 10.1038/nrn3200

Moss MB, Moore TL, Schettler SP, Killiany R, Rosene D, 2007. Successful vs. Unsuccessful Aging in the Rhesus Monkey, in: Riddle D (Ed.), Brain Aging: Models, Methods, and Mechanisms. CRC Press/Taylor & Francis, Boca Raton, FL.

Murman DL, 2015. The Impact of Age on Cognition. Semin. Hear 36, 111–121. 10.1055/s-0035-1555115 [PubMed: 27516712]

Nam S, Choi J, Yoo D, Kim W, Jung H, Kim J, Yoo M, Lee S, Kim C, Yoon Y, Hwang I, 2014. Effects of curcumin (Curcuma longa) on learning and spatial memory as well as cell proliferation and neuroblast differentiation in adult and aged mice by upregulating brain-derived neurotrophic factor and CREB signaling. J. Med. Food 17, 641–649. 10.1089/JMF.2013.2965 [PubMed: 24712702]

Page TL, Einstein M, Duan H, He Y, Flores T, Rolshud D, Erwin JM, Wearne SL, Morrison JH, Hof PR, 2002. Morphological alterations in neurons forming corticocortical projections in the neocortex of aged Patas monkeys. Neurosci. Lett. 317, 37–41. 10.1016/S0304-3940(01)02428-4 [PubMed: 11750991]

Parada E, Buendia I, Navarro E, Avendaño C, Egea J, López M, 2015. Microglial HO-1 induction by curcumin provides antioxidant, antineuroinflammatory, and glioprotective effects. Mol. Nutr. Food Res 59, 1690–1700. 10.1002/MNFR.201500279 [PubMed: 26047311]

Park L, Zhang H, Gibson G, 2001. Co-culture with astrocytes or microglia protects metabolically impaired neurons. Mech. Ageing Dev 123, 21–27. 10.1016/S0047-6374(01)00336-0 [PubMed: 11640948]

Peters A, 2009. The effects of normal aging on myelinated nerve fibers in monkey central nervous system. Front. Neuroanat 10.3389/neuro.05.011.2009

Peters A, Kemper T, 2012. A review of the structural alterations in the cerebral hemispheres of the aging rhesus monkey. Neurobiol. Aging 10.1016/j.neurobiolaging.2011.11.015

Peters A, Sethares C, Luebke JI, 2008. Synapses are lost during aging in the primate prefrontal cortex. Neuroscience 152, 970–981. 10.1016/j.neuroscience.2007.07.014 [PubMed: 18329176]

Plagenhoef M, Callahan P, Beck W, Blake D, Terry A, 2021. Aged rhesus monkeys: Cognitive performance categorizations and preclinical drug testing. Neuropharmacology 187. 10.1016/J.NEUROPHARM.2021.108489

Rainey-Smith S, Brown B, Sohrabi H, Shah T, Goozee K, Gupta V, Martins R, 2016. Curcumin and cognition: a randomised, placebo-controlled, double-blind study of community-dwelling older adults. Br. J. Nutr 115, 2106–2113. 10.1017/S0007114516001203 [PubMed: 27102361]

Rapp P, 1990. Visual discrimination and reversal learning in the aged monkey (Macaca mulatta). Behav. Neurosci 104, 876–884. 10.1037//0735-7044.104.6.876 [PubMed: 2285486]

Rinwa P, Kumar A, 2012. Piperine potentiates the protective effects of curcumin against chronic unpredictable stress-induced cognitive impairment and oxidative damage in mice. Brain Res. 1488, 38–50. 10.1016/J.BRAINRES.2012.10.002 [PubMed: 23099054]

Rodriguez A, Ehlenberger D, Kelliher K, Einstein M, Henderson SC, Morrison JH, Hof PR, Wearne SL, 2003. Automated reconstruction of three-dimensional neuronal morphology from laser scanning microscopy images. Methods 30, 94–105. 10.1016/S1046-2023(03)00011-2 [PubMed: 12695107]

Rodriguez A, Ehlenberger DB, Hof PR, Wearne SL, 2006. Rayburst sampling, an algorithm for automated three-dimensional shape analysis from laser scanning microscopy images. Nat. Protoc 1, 2152–2161. 10.1038/nprot.2006.313 [PubMed: 17487207]

Rozycka A, Liguz-Lecznar M, 2017. The space where aging acts: focus on the GABAergic synapse. Aging Cell. 10.1111/acel.12605

Salthouse T, 2012. Consequences of age-related cognitive declines. Annu. Rev. Psychol 10.1146/annurev-psych-120710-100328

Salthouse TA, 2009. When does age-related cognitive decline begin? Neurobiol. Aging 10.1016/j.neurobiolaging.2008.09.023

Salvioli S, Sikora E, Cooper EL, Franceschi C, 2007. Curcumin in cell death processes: A challenge for CAM of age-related pathologies. Evidence-based Complement. Altern. Med 10.1093/ecam/nem043

Sarker MR, Franks SF, 2018. Efficacy of curcumin for age-associated cognitive decline: a narrative review of preclinical and clinical studies. GeroScience. 10.1007/s11357-018-0017-z

Shobin E, Bowley MP, Estrada LI, Heyworth NC, Orczykowski ME, Eldridge SA, Calderazzo SM, Mortazavi F, Moore TL, Rosene DL, 2017. Microglia activation and phagocytosis: relationship with aging and cognitive impairment in the rhesus monkey. GeroScience 39, 199–220. 10.1007/s11357-017-9965-y [PubMed: 28238188]

Sholl DA, 1953. Dendritic organization in the neurons of the visual and motor cortices of the cat. J. Anat 87, 387–406. [PubMed: 13117757]

Sikora E, Bielak-Zmijewska A, Mosieniak G, Piwocka K, 2010a. The Promise of Slow Down Ageing May Come from Curcumin. Curr. Pharm. Des 16, 884–892. 10.2174/138161210790883507 [PubMed: 20388102]

Sikora E, Scapagnini G, Barbagallo M, 2010b. Curcumin, inflammation, ageing and age-related diseases. Immun. Ageing 10.1186/1742-4933-7-1

Stacchiotti A, Corsetti G, 2020. Natural Compounds and Autophagy: Allies Against Neurodegeneration. Front. cell Dev. Biol 8. 10.3389/FCELL.2020.555409

Styr B, Gonen N, Zarhin D, Ruggiero A, Atsmon R, Gazit N, Braun G, Frere S, Vertkin I, Shapira I, Harel M, Heim L, Katsenelson M, Rechnitz O, Fadila S, Derdikman D, Rubinstein M, Geiger T, Ruppin E, Slutsky I, 2019. Mitochondrial Regulation of the Hippocampal Firing Rate Set Point and Seizure Susceptibility. Neuron 102, 1009–1024.e8. 10.1016/J.NEURON.2019.03.045 [PubMed: 31047779]

Tegenge MA, Rajbhandari L, Shrestha S, Mithal A, Hosmane S, Venkatesan A, 2014. Curcumin protects axons from degeneration in the setting of local neuroinflammation. Exp. Neurol 253, 102–110. 10.1016/j.expneurol.2013.12.016 [PubMed: 24382451]

Tigges J, Gordon T, McClure H, Hall E, Peters A, 1988. Survival rate and life span of rhesus monkeys at the Yerkes regional primate research center. Am. J. Primatol 15, 263–273. 10.1002/AJP.1350150308 [PubMed: 31968890]

Uğuz A, Öz A, Nazıroğlu M, 2016. Curcumin inhibits apoptosis by regulating intracellular calcium release, reactive oxygen species and mitochondrial depolarization levels in SH-SY5Y neuronal cells. J. Recept. Signal Transduct. Res 36, 395–401. 10.3109/10799893.2015.1108337 [PubMed: 26608462]

Uryash A, Flores V, Adams J, Allen P, Lopez J, 2020. Memory and Learning Deficits Are Associated With Ca 2+ Dyshomeostasis in Normal Aging. Front. Aging Neurosci 12. 10.3389/FNAGI.2020.00224

Voulgaropoulou S, van Amelsvoort T, Prickaerts J, Vingerhoets C, 2019. The effect of curcumin on cognition in Alzheimer's disease and healthy aging: A systematic review of pre-clinical and clinical studies. Brain Res. 1725. 10.1016/J.BRAINRES.2019.146476

Wang M, Gamo N, Yang Y, Jin L, Wang X, Laubach M, Mazer J, Lee D, Arnsten A, 2011. Neuronal basis of age-related working memory decline. Nature 476, 210–213. 10.1038/NATURE10243 [PubMed: 21796118]

Wang X, Michaelis EK, 2010. Selective neuronal vulnerability to oxidative stress in the brain. Front. Aging Neurosci 10.3389/fnagi.2010.00012

Williams IM, Wallom K-L, Smith DA, Al Eisa N, Smith C, Platt FM, 2014. Improved neuroprotection using miglustat, curcumin and ibuprofen as a triple combination therapy in Niemann–Pick disease type C1 mice. Neurobiol. Dis 67, 9–17. 10.1016/j.nbd.2014.03.001 [PubMed: 24631719]

Xekardaki A, Kövari E, Gold G, Papadimitropoulou A, Giacobini E, Herrmann F, Giannakopoulos P, Bouras C, 2015. Neuropathological Changes in Aging Brain, in: Advances in Experimental Medicine and Biology. Springer New York LLC, pp. 11–17. 10.1007/978-3-319-08939-3_6

Yang Z, Zhao T, Zou Y, Zhang JH, Feng H, 2014. Curcumin inhibits microglia inflammation and confers neuroprotection in intracerebral hemorrhage. Immunol. Lett 160, 89–95. 10.1016/j.imlet.2014.03.005 [PubMed: 24680995]

Highlights:

- Spatial working memory (WM) performance begins to decline in middle age
- Pyramidal neurons exhibit hyperexcitability and spine loss beginning in middle age
- Curcumin-treated subjects exhibit better WM ability and less neuronal excitability

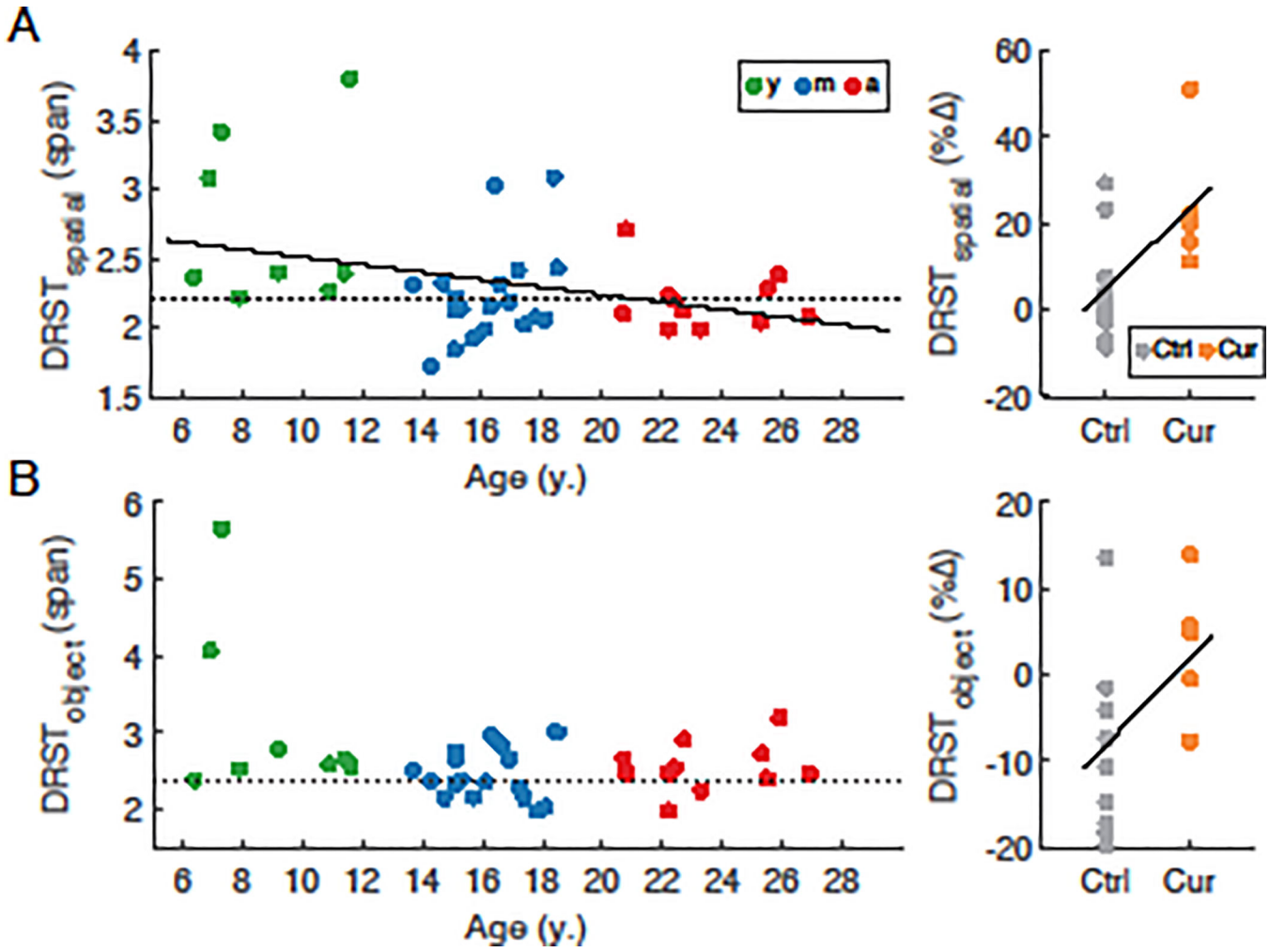

Fig. 1. Performance of individual subjects on the Delayed Recognition Span Task.

(A) *left:* DRST-Spatial span vs. age in young (y, green), middle-aged (m, blue), and aged (a, red) subjects; *right:* greater improvement in DRST-Spatial span in the curcumin-treated middle-aged cohort. (B) *left:* DRST-Object span in the same cohort of monkeys as in (A); *right:* greater improvement in DRST-object span in the curcumin-treated middle-aged cohort. Dotted lines denote performance threshold below which subjects are classified as impaired on each task. Solid lines denote statistically significant regressions ($p<0.05$). Data were obtained from a total of 8 young, 19 middle-aged control, 12 aged, and 7 middle-aged curcumin-treated monkeys.

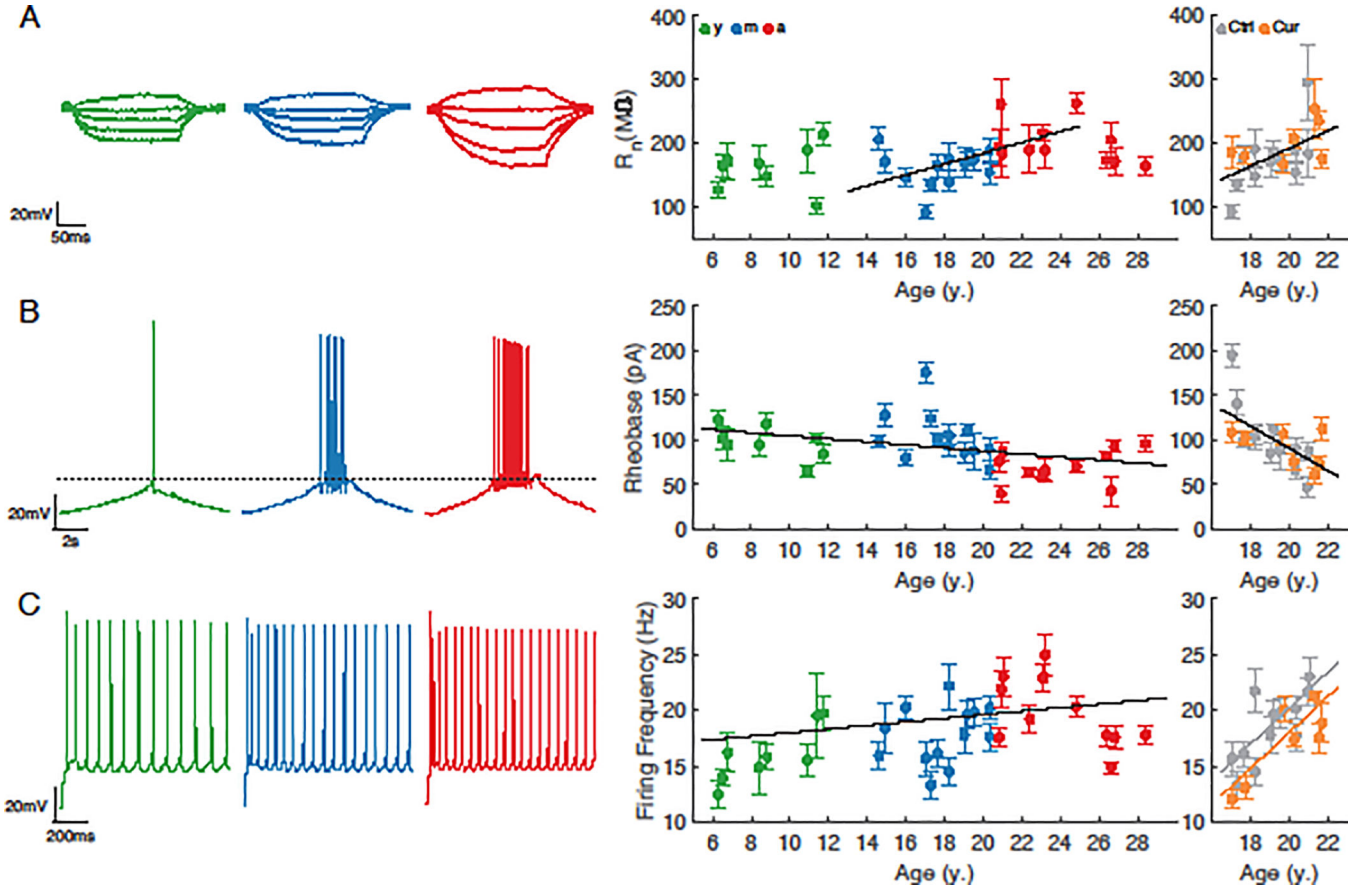

Fig. 2. Electrophysiological properties of LPFC neurons across the adult lifespan and effect of curcumin treatment in middle-aged subjects.

(A) *left:* Voltage responses of representative neurons in each age group to a series of hyper- and de-polarizing current steps; *middle:* input resistance (R_n) vs. age for neurons from each age group, and *right:* from middle-aged monkeys +/− curcumin. (B) *left:* Voltage responses of representative neurons in each age group to a current ramp protocol; *middle:* rheobase vs. age for neurons from each age group, and *right:* from middle-aged monkeys +/− curcumin. (C) *left:* Voltage responses of representative neurons in each age group to a 2s 280pA current step; *middle:* firing rate in response to a 280pA step vs. age for neurons from each age group, and *right:* from middle-aged monkeys +/− curcumin. Data shown as mean ±SEM for each monkey. Regressions include subject as random effect. Solid lines denote statistically significant regressions ($p<0.05$). $n = 8$ young, 13 middle-aged control, 11 aged, and 7 middle-aged curcumin-treated animals ($n = 86$, 190, 102 and 135 neurons, respectively).

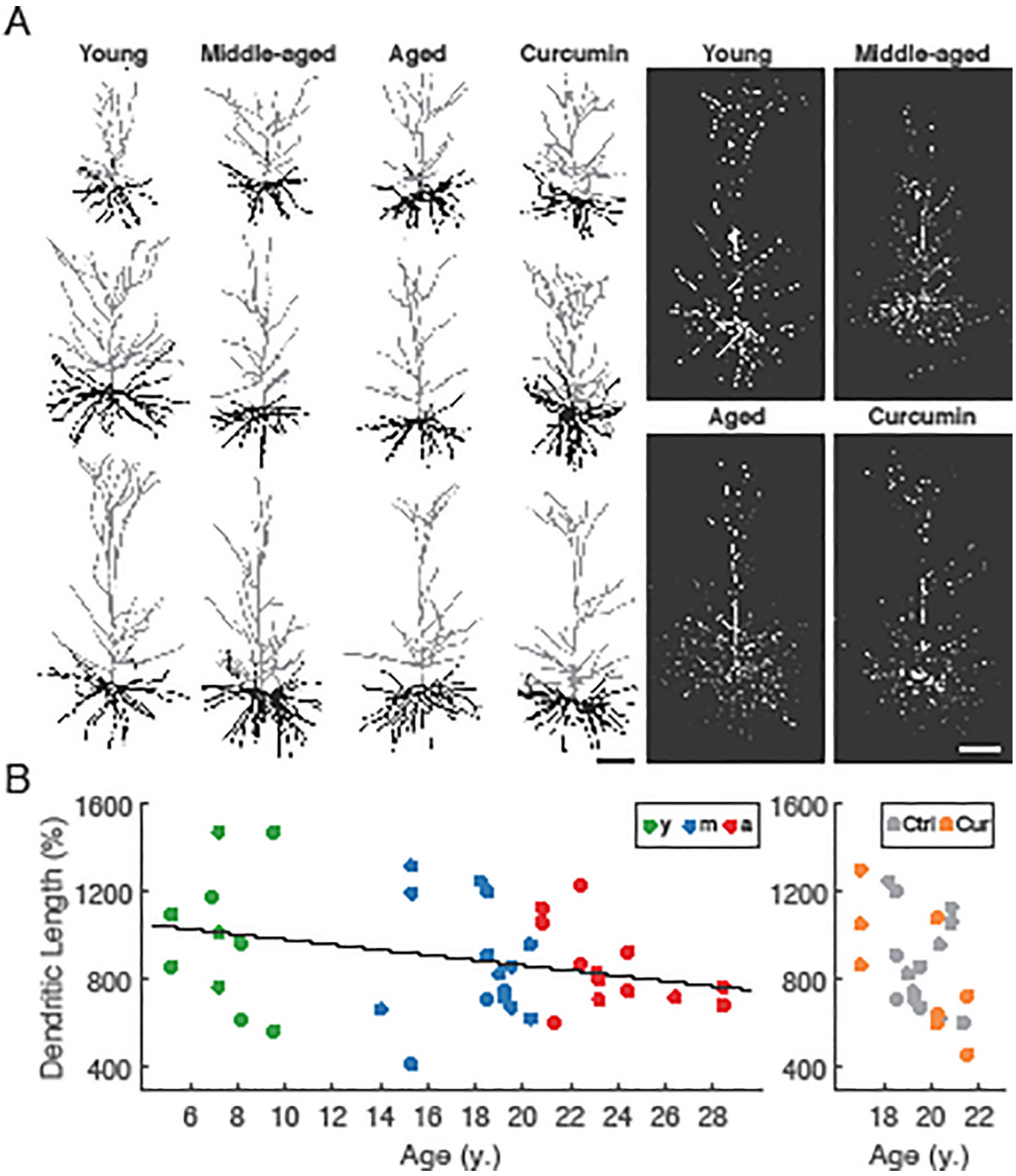

Fig. 3. Dendritic properties of LPFC neurons across the adult lifespan and effect of curcumin treatment in middle-aged subjects.

(A) *left:* Reconstructions of representative L3 pyramidal neurons in each group; *right:* representative confocal images of L3 pyramidal neurons. (B) *left:* Normalized apical dendritic length vs. age for neurons from each age group, and *right:* from middle-aged monkeys +/− curcumin (% = 100*dendritic length/soma-to-pia distance). Solid line denotes statistically significant regression ($p<0.05$). $n = 5$ young, 9 middle-aged control, 7 aged, and 3 middle-aged curcumin-treated animals ($n = 11$, 16, 13 and 8 neurons, respectively).

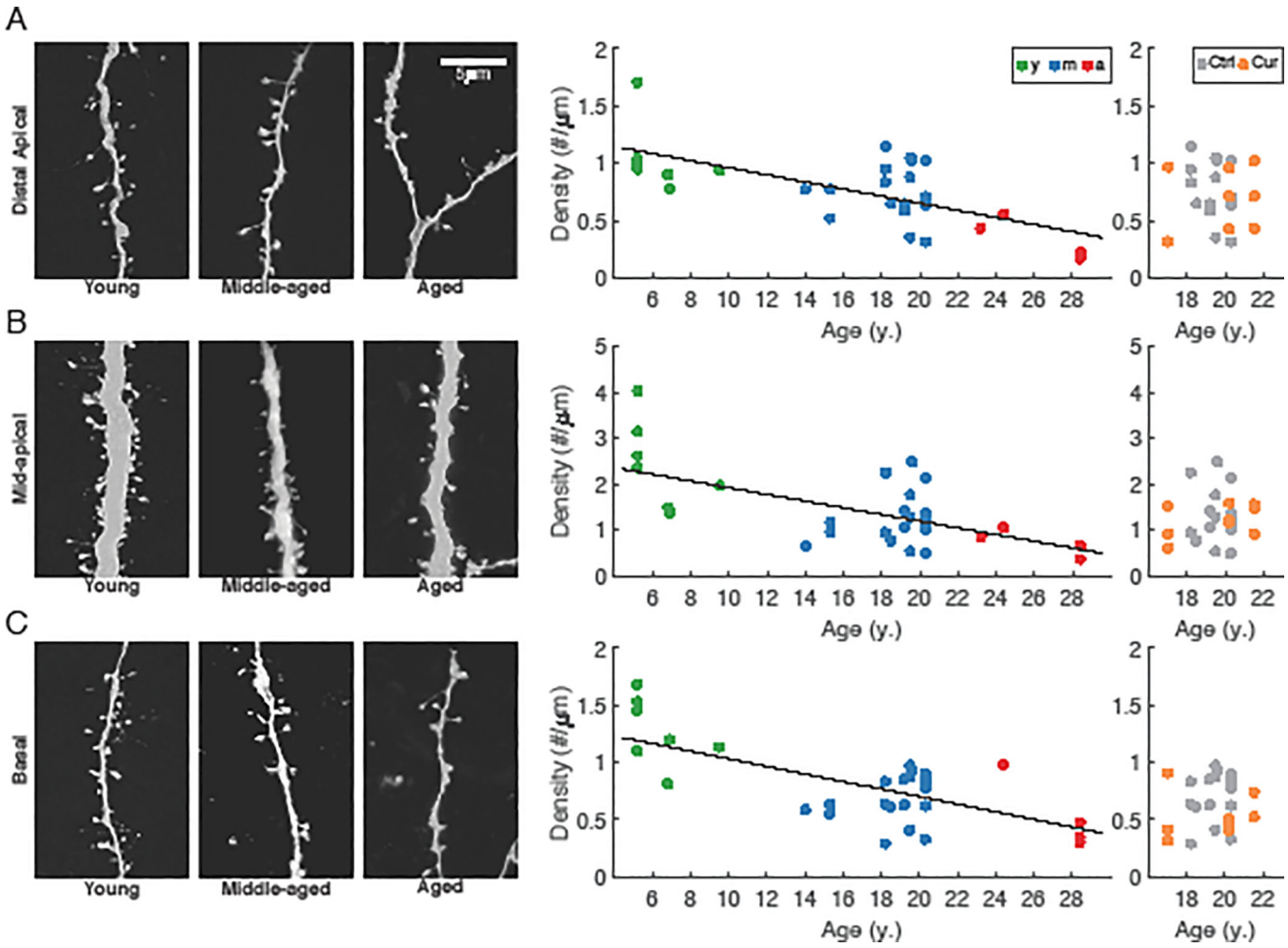

Fig. 4. Dendritic spine densities of LPFC neurons across the adult lifespan and effect of curcumin treatment in middle-aged subjects.

(A) *left:* Representative dendritic segments with spines in the distal apical dendritic arbors of young, middle-aged, and aged subjects; *middle:* distal apical spine density vs. age for neurons from each age group, and *right:* from middle-aged monkeys +/− curcumin. (B) *left:* Representative dendritic segments with spines in the mid-apical dendritic arbors of young, middle-aged, and aged subjects; *middle:* mid-apical spine density vs. age for neurons from each age group, and *right:* from middle-aged monkeys +/− curcumin. (C) *left:* Representative dendritic segments with spines in the basal dendritic arbors of young, middle-aged, and aged subjects; *middle:* basal spine density vs. age for neurons from each age group, and *right:* from middle-aged monkeys +/− curcumin. Solid lines denote statistically significant regression ($p<0.05$). $n = 4$ young, 10 middle-aged control, 3 aged, and 3 middle-aged curcumin-treated animals ($n = 7$, 19, 5 and 9 neurons, respectively).

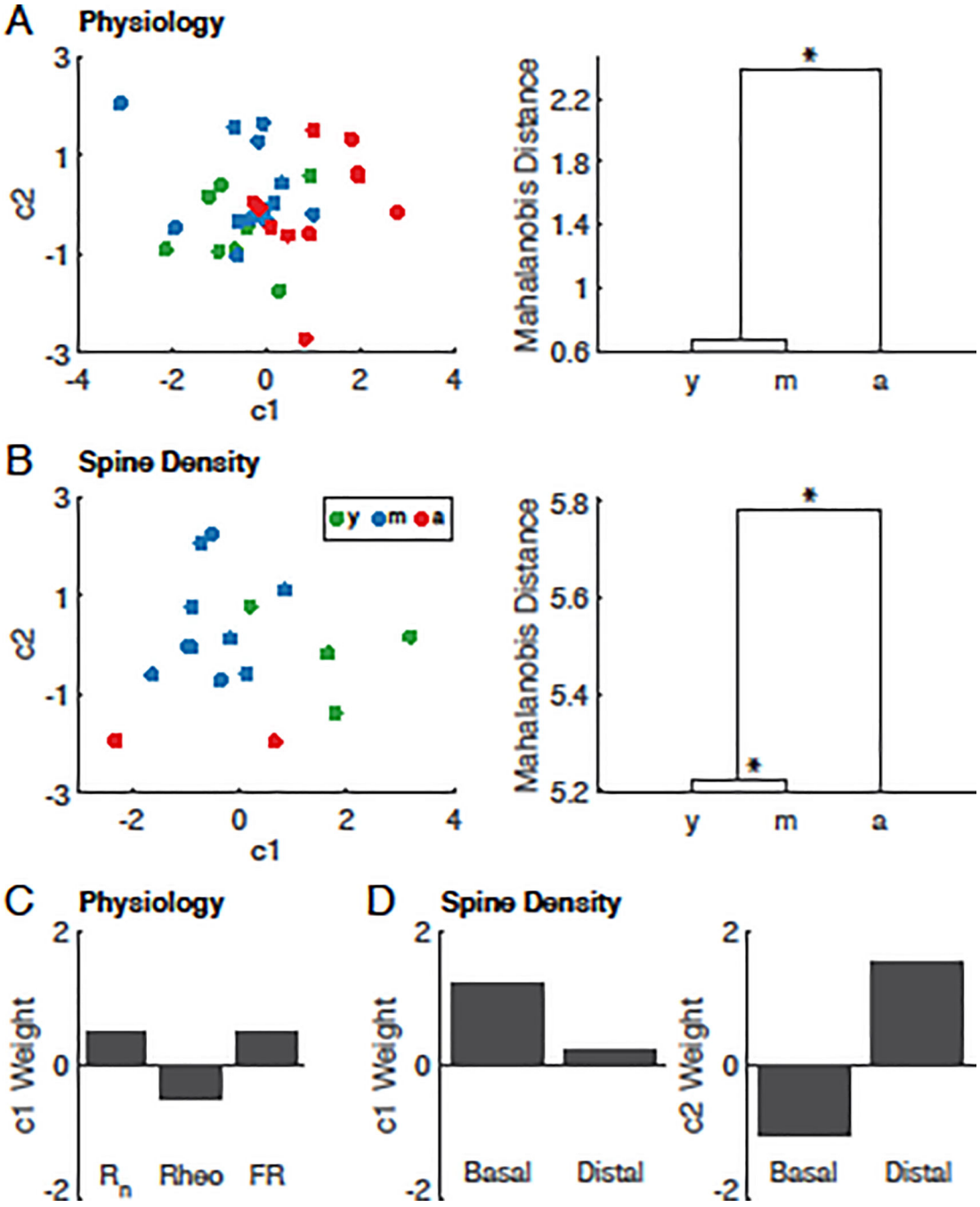

Fig. 5. MANOVA for between-age group relationships of physiological properties, and spine density of LPFC neurons.

MANOVA of L3 pyramidal neuronal (A) physiological properties and (B) spine density showing resulting scatter plots of the first two canonical variables of animals from each age group (left panels) and dendrograms of group mean clusters (right panels), with the height representing the shortest Mahalanobis distance between clusters. (C) Component weights of input resistance (R_n), rheobase (rheo) and firing rate in response to a 280pA step (FR) for the first canonical variable (c1) in (A). (D) Component weights of basal and distal-apical

(Distal) spine density for the first (c1, *left*) and second (c2, *right*) canonical variables in (B). Statistically significant dimensions tested with Wilks' lambda test statistic. * denotes $p<0.05$